ELSEVIER

Polymer 43 (2002) 4571–4583

polymer

www.elsevier.com/locate/polymer

Amorphous cell studies of polyglycolic, poly(L-lactic), poly(L,D-lactic) and poly(glycolic/L-lactic) acids

J. Blomqvist[a,*], B. Mannfors[a,1], L.-O. Pietilä[b,2]

[a]*Department of Physical Sciences, FIN-00014, University of Helsinki, P.O. Box 64, Helsinki, Finland*
[b]*Laboratory of Polymer Chemistry, Department of Chemistry, FIN-00014, University of Helsinki, P.O. Box 55, Helsinki, Finland*

Received 5 April 2001; received in revised form 24 April 2002; accepted 13 May 2002

Abstract

In this paper static amorphous state properties (solubility parameter, free volume (using the Voorintholt method and the Voronoi tessellations) and pair correlation functions, the last ones also by including water molecules in the cells), which can be related to the probability for water uptake, have been studied for polyglycolic (PGA), poly(L-lactic) (PLLA), poly(L,D-lactic) (PLLA/PDLA) and poly(glycolic/L-lactic) (PGA/PLLA) acids, known to be biodegradable polymers. The polymer consistent force field, as modified by the authors, has been used in the calculations. The main purpose of this paper is to investigate, which of the amorphous state properties would be relevant for water uptake. We also discuss the validity of th6e methods used for these kinds of studies, and the related reliability of the computed results. Chain flexibilities of the studied polyesters in the amorphous phase have been analyzed, and the intermolecular interactions are found to cause the most significant variations in the distributions of the adjacent chain dihedral angle pairs and in the related populations of the low-energy regions of the comonomers. The solubility parameters, as calculated from the cohesion energy densities of the constructed models, suggest PGA being most compatible with water, in agreement with experiments. On the other hand, the quantitative structure–property relationships method 'Synthia' suggests a very similar solubility in water for all particular polyesters. In the PLAs and PGA/PLLA, however, a larger number of hydrogen bonds is formed between the water molecules and the carbonyl oxygen atoms of the chains showing a better possibility of PLLA and its copolymers to break into shorter chains. As an explanation, the hydrophobic methyl groups of the lactide units are suggested to push the water molecules closer to the carbonyl groups than in homo-PGA.

Keywords: Amorphous cell; Aliphatic polyesters; Water uptake

1. Introduction

Polyglycolic acid (PGA) (R = H) and poly(L-lactic) acid (PLLA) (R = CH_3)

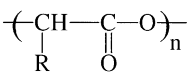

as well as their copolymers, namely copolymers of L- and D-lactide units (PLLA/PDLA) and of L-lactide and glycolide units (PGA/PLLA), are important polyesters due to their known biodegradability. They are therefore widely studied [1–12], and used in, for example, biomedical applications, such as in surgical sutures, bone fixation devices and in drug delivery system in pharmacology (see Refs. [1–3,12], and references therein). Other applications include paper coatings, food packaging and film wraps [2,12].

In experimental studies on PGA and PLLA (intrinsically semicrystalline with a typical crystallinity of about 50 and 40%, respectively [4]), it has been found that the biodegradation process first takes place in the amorphous phase of the polymer [3,12], leading to an increase in crystallinity of polymer materials [3,5]. Polymer chains in an amorphous state first degrade by hydrolysis into shorter chains, after which metabolization takes place also in the crystalline region [3,5]. Kister et al. [1] found that also the tacticity of the polymer chains affects a polymer's degradation kinetics. Copolymerization is known to reduce the long-range order in a material, thus improving biodegradability, and, for example, the more crystalline homo-PGA and PLLA degrade more slowly than do the

* Corresponding author. Fax: +358-9-191-50610.
E-mail address: johanna.m.blomqvist@helsinki.fi (J. Blomqvist).
[1] Present address: Biophysics Research Division, University of Michigan, 930 N. University Avenue, Ann Arbor, MI 48109, USA.
[2] Present address: VTT Processes, P.O. Box 1401, FIN-02044 VTT, Finland.

0032-3861/01/$ - see front matter
PII: S0032-3861(02)00312-9

copolymers of PGA and PLLA [6,7]. The hydrophilic/hydrophobic balance was also found to have an impact on the degradation rate [6]. The hydrolytic degradation of copolymers of PGA and PLLA, and of PLLA and PDLA has experimentally been studied also in Refs. [8–10].

In the present paper, such static amorphous state properties, which can be related to the probability of water uptake by PGA, PLLA, PLLA/PDLA and PGA/PLLA, are studied by constructing amorphous cell models for these polyesters. The generated cell structures were examined by calculating X-ray scattering curves and distributions of the adjacent chain ($C(sp^3)$–$C(sp^2)$, $C(sp^3)$–$O(sp^3)$) dihedral angle pairs. The pair correlation functions (PCFs), without and with water molecules in the cells, and the solubility parameters were computed to investigate the ability of the studied polyesters to react with water. The free volumes were calculated to consider the packing of the materials and the Voronoi tessellations to study the free volume distribution in the constructed amorphous structures. The exact chain configurations in any of the samples used in experimental studies of a copolymer of L- and D-lactide units, was not known [11], for which reason simulations in this paper were carried out for a copolymer of (50%, 50%) alternating L- and D-lactide units and for a random (50%, 50%) copolymer of L,D- and D,L-dyads, as well as for a random (50%, 50%) copolymer of L-lactide and glycolide units. The main purpose of this work however has been to study, which of the static amorphous phase properties are relevant for water uptake by these polyesters. Also the approximations in the methods, and the reliability of the results due to these approximations, are discussed.

2. Computational details

All calculations were performed by the Amorphous Cell module of MSIs InsightII/Discover software [13] on an SGI Origin 2000 supercomputer at the Center for Scientific Computing (CSC, Espoo, Finland). Also some in-house codes were used in the analysis of the results. All graphics presented here have been printed out from InsightII.

Molecular mechanics (MM) and molecular dynamics (MD) calculations were carried out using the polymer consistent force field (PCFF) [14–21], modified by the authors in Refs. [22,23] to correctly produce the torsional statistics of the $C(sp^2)$–$O(sp^3)$, $C(sp^3)$–$O(sp^3)$ and $C(sp^3)$–$C(sp^2)$ bonds in the kind of polyesters considered in this paper. Especially for the energy behavior of the $C(sp^3)$–$C(sp^2)$ rotation, the non-modified PCFF gave results which were in severe disagreement with our corresponding quantum chemical MP2/6-31G(d) ones as well as with the results from the observed conformational states [24]. The modified PCFF was further tested in Refs. [25,26], and found to give realistic single chain properties, as calculated by the RIS Metropolis Monte Carlo method [27], for the selected main chain polyesters including PGA and PLAs, as well as for a few side group polyesters.

Construction of the amorphous state model is based on the knowledge of the inter- and intramolecular interactions between atoms, as given by the force field model used. Macroscopic properties of real polymers, however, depend on the crystallinity of the polymer, mutual orientation of polymer chains, and cross-linking of the material, and it has to be emphasized that our constructed models are valid only for a fully amorphous, isotropic, non-oriented and non-cross-linked polymer phase. There are several factors that also influence the final generated structure of the cells. The most crucial ones are the selected force field, packing density and temperature, cut-off for non-bonded interactions and the size of the cell. Especially the force field, used for energy determinations in the simulations, is of decisive importance since the detailed structure of the chain and further the local structure and packing of a bulky material are based on the model of atom–atom interactions.

The amorphous polymer models were built with the Theodorou and Suter method [28,29] using periodic boundary conditions and the minimum image convention [30]. In generation of the cells the modified PCFF [22,23] was used to determine the values for the dihedral angles of the added bonds. The cells were first generated with a density lower than the observed one to obtain more realistic initial conformational states. (This approach also reduces the number of MD steps needed to equilibrate the structures.) The temperature was set to that of experimental studies (298 K). Several different structures were constructed for all polyesters to obtain sufficient statistics for averaging of the computed properties of interest. Thus, for homo-polymers 10 amorphous cells containing five identical chains with a chain length of 50 repeat units were built. Since the differences in the final optimized cells were small, only four cells but with five dissimilar chains were built for the copolymers, to obtain sufficiently random structures. The constructed initial structures had large potential energies, and the cells contained regions in which the density fluctuated a lot. The structures were therefore optimized using alternating MM minimization (using the conjugate gradient method) and MD equilibration (with velocity Verlet algorithm) to achieve a more homogenous distribution of atoms in the cells. The NVT ensemble was used in the MD simulations, with a higher temperature of 500 K to avoid trapping in high-energy minima, and with a group-based cut-off value of 7 Å for non-bonded interactions (in these initial steps a smaller cut-off value than that used in the final relaxation of the systems was chosen to reduce the CPU time). In the initial steps also the torsion and non-bonded parameters of the force field were scaled to half of their real values in order to facilitate the relaxation. Typically, 1000 MM and 10 000 MD steps (with a time step of 1 fs) were used in one cycle, and usually 5–10 cycles were needed to achieve statistically stable configurations. When the system was relaxed (i.e. the cohesive energy

Table 1
Calculated and experimental densities (in g/cm^3), calculated CEDs (in J/m^3) and total energies (in kcal/mol) of the refined amorphous cells of PGA, PLLA, PLLA/PDLAs, and PGA/PLLA, respectively

	PGA	PLLA	Alternating PLLA/PDLA	Random PLLA/PDLA	Random PGA/PLLA
Density					
	1.50[a]	1.25[a]	1.25[a]	1.25[a]	1.375[a]
Experimental	1.50[b]	1.248[c]	1.248[c]	1.248[c]	1.374[d]
QSPR[e]	1.477	1.254	1.254	1.254	1.345
CED ($\times 10^8$)	11.55	4.86	5.39	5.49	7.08
Energy					
Cell 1	1141.7	1676.4	2787.0	2711.6	1165.9
Cell 2	1100.3	1640.1	2764.7	2767.0	1127.6
Cell 3	1132.0	1626.2	2771.4	2760.7	1129.0
Cell 4	1133.4	1642.2	2727.9	2734.3	1172.1
Cell 5	1159.6	1615.2	–[f]	–[f]	–[f]
Cell 6	1088.5	1665.4	–[f]	–[f]	–[f]
Cell 7	1061.7	1606.5	–[f]	–[f]	–[f]
Cell 8	1063.3	1579.5	–[f]	–[f]	–[f]
Cell 9	1148.2	1661.7	–[f]	–[f]	–[f]
Cell 10	1156.8	1642.0	–[f]	–[f]	–[f]
Average	1118.6 ± 49.0	1635.5 ± 48.5	2762.8 ± 29.6	2744.1 ± 29.2	1148.7 ± 22.2

[a] Used in simulations of this study.
[b] Ref. [31].
[c] Ref. [32].
[d] Average value of the experimental densities of PGA and PLLA.
[e] Refs. [13,33].
[f] Four cells containing five dissimilar chains were constructed instead of 10 cells with five identical chains.

densities of the cells did no longer get larger, and the energies of the different cells were close to each other), the densities of the cells were increased to the experimental ones, i.e. 1.50 g/cm^3 for PGA [31], 1.25 g/cm^3 for the PLAs [32] and 1.375 g/cm^3 for PGA/PLLA (average of the first two). The temperature was set to the experimental value of 298 K, the cut-off value to 11 Å (i.e. less than a half of the cell-edge length due to the minimum image convention approach in the MD simulations) and the correct (non-scaled) torsion and non-bonded parameters were used. Tail corrections [30] were included in these calculations. The configurations were then again relaxed after which the properties of interest were computed as average values of all constructed cells for all studied polyesters.

3. Results and discussion

After the final structure refinement, the cells were evenly filled and the edges of the cubic cells were 24.91 Å for PGA, 28.82 Å for the PLAs, and 26.97 Å for PGA/PLLA. The (total) energies of the cells, which are given in Table 1 with the densities and cohesion energy densities (CEDs), were close to each other for each polymer, and they came out (in kcal/mol) as 1119 ± 49 for PGA, 1636 ± 49 for PLLA, 2763 ± 30 for alternating PLLA/PDLA, 2744 ± 29 for random PLLA/PDLA, and 1149 ± 22 for random PGA/PLLA. Although not the only factor, the computed CEDs can be used to estimate how much energy/volume is needed to break intermolecular contacts in the studied amorphous structures. PGA, as having the largest CED, would need the largest amount of energy whereas PLLA and the PLLA/PDLAs would need the smallest amount of energy, PGA/PLLA needing somewhat more energy than the PLAs. It is interesting to note that this order of 'stability' is in agreement with the observed tensile strengths [32]. The densities given by the computationally fast quantitative structure–property relationships (QSPR) method [33] were all close to the experimental densities. It has to be noted, however, that the QSPR method does not take tacticity into account. (The QSPR method is available in the Synthia-module of the InsightII/Discover software package [13], and it estimates various polymer properties using derived correlations between properties and connectivity indices [33].)

3.1. Validation calculations

The constructed cell structures were examined by calculating the X-ray scattering curves and the distributions of the adjacent chain dihedral angle pairs. The calculated X-ray scattering curves (with Cu K_α radiation) of PGA, PLLA and the PLLA/PDLAs are presented in Fig. 1, and the peaks are given in Table 2 together with the existing experimental data (for PLLA and random PLLA/PDLA [1,8]). The broad diffusion bands, seen in the figure, are typical of amorphous polymeric materials, and indicate good

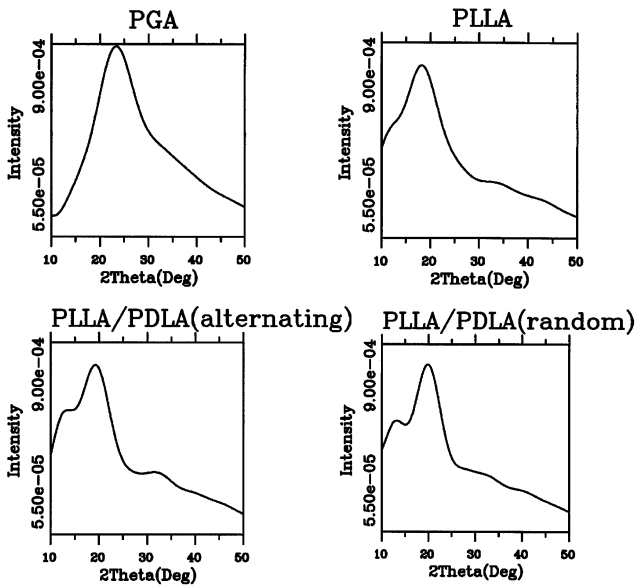

Fig. 1. Calculated X-ray scattering curves of PGA, PLLA and PLLA/-PDLAs.

amorphous performance of the constructed models. In fact, all calculated scattering curves are very similar, having the highest peak at $2\theta \approx 18-23°$, and a broad shoulder at $2\theta \approx 28-35°$. The PLLA and PLLA/PDLAs have an additional shoulder at $2\theta = 10-15°$. The atom–atom distances can also be obtained from the PCFs, though in this paper we only give the distances between the carbonyl oxygen and other atoms, the main interest of the paper being in water uptake. As can be seen from Table 2, the calculated scattering curves are in good agreement with the existing experimental data.

The distributions of the populated conformations are given in Fig. 2 for the adjacent $C(sp^3)-C(sp^2)$ and $C(sp^3)-O(sp^3)$ rotations in PGA and PLLA, and separately in the glycolide, and D- and L-lactide units of the PLLA/PDLAs and PGA/PLLA (the $C(sp^2)-O(sp^3)$ rotation is restricted, and as having a well-defined *trans* minimum does not affect the populations of the $C(sp^3)-C(sp^2)$ and $C(sp^3)-O(sp^3)$ energy states). In order to have pictures, which directly can be compared with each other, the distributions given for PGA and PLLA have been taken from four such cells, which represent best the amorphous phase of these polymers, though 10 cells altogether were constructed for homo-polymers. The same rotations were studied in the model molecules of PGA and PLLA in Ref. [23]. Comparing the results it can be seen that the populated conformations of the constructed amorphous structures fall into the same minimum energy regions as shown in the potential energy maps of individual model molecules [23], and that the distributions for the corresponding repeat units are qualitatively similar in each case. As regards intramolecular interactions, this indicates that the ester groups, which are between the CHR (R = H or CH_3) subgroups, hinder interactions between the CHR groups. However, the points are scattered all over the minimum energy regions, also over the transition regions between the minima of the $C(sp^3)-C(sp^2)$ rotation. The net intermolecular interactions thus are significant enough as compared to the low-energy $C(sp^3)-C(sp^2)$ barriers to change the conformations of the chains in the constructed amorphous structures from those in isolated chains.

The average populations (in %) of the conformational low-energy regions are given in Table 3 for the glycolide and lactide units in PGA, PLLA, alternating and random PLLA/PDLA and random PGA/PLLA. Here, all constructed cells (i.e. 10 cells for each homo-polymer and four cells for each copolymer) have been utilized. Table 3 shows that the populations of the corresponding units in the copolymers are mostly rather close to those of homo-PGA and PLLA. (Note that the D- and L-lactide contributions in homo-PLLA and PDLA would be mirror images of each other with respect to the $C(sp^3)-O(sp^3)$ rotation.) Concerning interactions along the chain this is as expected, since the particular dihedral angle pairs in adjacent monomer units are separated by rigid $C(sp^2)-O(sp^3)$ bonds. Neither do the interactions through

Table 2
Peaks in calculated X-ray scattering curves of PGA, PLLA and PLLA/PDLAs

	Intensity/10^{-4}	Location 2θ/°	Experimental
PGA	8.9047	23.3	–
		30–35 (sh)	–
PLLA[a]		10–15 (sh)	10–14 (sh)
	8.0154	18.2	16–20
		30–35 (sh)	30–36 (sh)
Alternating PLLA/PDLA		12–15 (sh)	–
	8.0069	19.2	–
		28–33 (sh)	–
Random PLLA/PDLA[a,b]		12–15 (sh)	12–14 (sh), ~12 (sh)
	8.0922	19.9	16–18, 17–19
		30–35 (sh)	30–36 (sh), 30–36 (sh)

sh, shoulder.
[a] Experimental values from Ref. [1].
[b] Experimental values from Ref. [8].

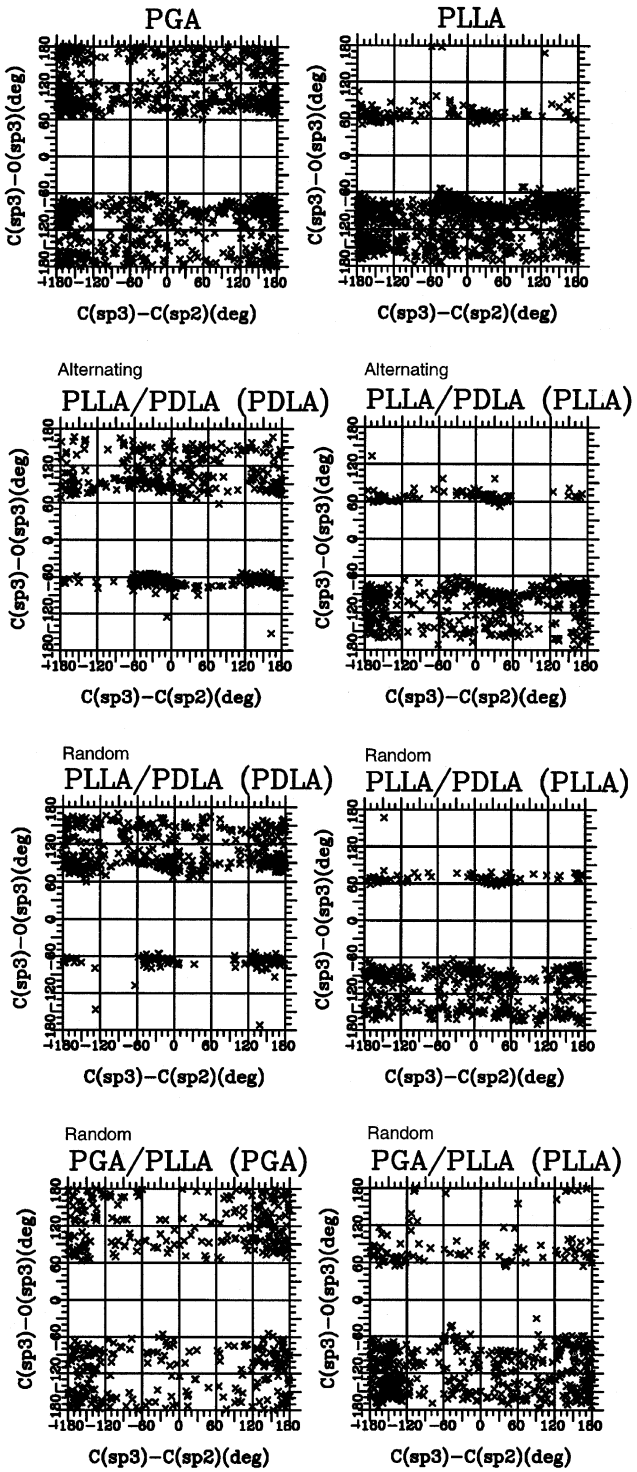

Fig. 2. Calculated distributions of the adjacent chain $C(sp^3)$–$C(sp^2)$ and $C(sp^3)$–$O(sp^3)$ dihedral angle pairs of PGA and PLLA, of the D- and L-lactide units of PLLA/PDLAs and of the glycolide and L-lactide units of PGA/PLLA. The results are from four cells for each polymer to produce comparable pictures.

space significantly affect the populations, as given by the force field model used. Overall, with comparison to homo-PGA and PLLA, the highly populated (t, t) and (t, g) regions of the glycolide units in PGA/PLLA have gained

Table 3
Average population (in %) of the low-energy regions of PGA, PLLA, of the D- and L-lactide units of PLLA/PDLAs and of the glycolide and L-lactide units of PGA/PLLA in the optimized amorphous structures

Minimum	Rotation		Population
	$C(sp^3)$–$C(sp^2)$[a]	$C(sp^3)$–$O(sp^3)$[b]	
PGA			
Min1	t	t	28.2
Min2	t	g^+	26.1
Min3	t	g^-	24.8
Min4	c	g^+	10.3
Min5	c	g^-	10.6
PLLA			
Min1	t	g^+	6.4
Min2	t	g^-	49.8
Min3	c	g^+	5.7
Min4	c	g^-	38.1
Alternating PLLA/PDLA			
D-lactide units			
Min1	t	g^+	22.5
Min2	t	g^-	15.9
Min3	c	g^+	30.7
Min4	c	g^-	30.9
L-lactide units			
Min1	t	g^+	8.1
Min2	t	g^-	46.6
Min3	c	g^+	10.2
Min4	c	g^-	35.1
Random PLLA/PDLA			
D-lactide units			
Min1	t	g^+	47.4
Min2	t	g^-	13.3
Min3	c	g^+	31.9
Min4	c	g^-	7.4
L-lactide units			
Min1	t	g^+	7.4
Min2	t	g^-	44.2
Min3	c	g^+	8.6
Min4	c	g^-	39.8
Random PGA/PLLA			
Glycolide units			
Min1	t	t	29.6
Min2	t	g^+	27.4
Min3	t	g^-	26.7
Min4	c	g^+	8.9
Min5	c	g^-	7.4
Lactide units			
Min1	t	g^+	11.0
Min2	t	g^-	60.2
Min3	c	g^+	4.5
Min4	c	g^-	24.3

If the range (t, c, g^+, g^-) is given with $\phi_{min} > \phi_{max}$ (in degrees), it contains the 180° boundary. Division of the population into separate regions in the table is based on the location and size of the low-energy regions in the potential energy maps calculated for the same rotations in the model molecules of PGA and PLLA in Ref. [23].

[a] $c = (\phi_{min} = -90°, \phi_{max} = 90°)$, $t = (90°, -90°)$ (Note: $t = (-180°, 180°)$ in Min1 of PGA and in the glycolide units of random PGA/PLLA).

[b] In the glycolide units: $g^- = (\phi_{min} = -150°, \phi_{max} = -30°)$, $g^+ = (30°, 150°)$, $t = (150°, -150°)$, and in the lactide units: $g^- = (\phi_{min} = -180°, \phi_{max} = -30°)$, $g^+ = (30°, 180°)$ (there are no (*trans*, *trans*) minima in PLAs).

somewhat (4.6%) population, the (t, g) regions of the L-lactide units being much more populated (gain of 15.0%) and the (c, g) regions correspondingly less populated. The glycolide part thus seems to have a much stronger effect on the population of its comonomer than what the lactide part has. In the PLLA/PDLAs, the (t, g) regions of the L-lactide units lose population, the (c, g) regions gaining it, somewhat more in random PLLA/PDLA than in alternating PLLA/PDLA. On the other hand, the respective changes in the D-lactide units in alternating PLLA/PDLA are very different from those of the L-lactide part, the population of the (t, g) regions decreasing as much as 17.8%. In alternating PLLA/PDLA, where the regular distribution of the L and D units makes the polymer syndiotactic, the effect of the L-lactide component on the population of the D component is very significant, but not vice versa. In random PLLA/PDLA, which is an atactic polymer, both the L and D populations are much more similar to those of the respective homo-polymers. Variations due to different molecular arrangements in preferentially isotactic, syndiotactic and atactic PLAs were seen, for example, in the Raman and IR spectra, especially in the frequencies and intensities of the CH and methyl CH_3 bending modes [1]. The authors found two weak broad bands at 1336 and 1320 cm^{-1} in the Raman spectrum of preferentially syndiotactic PLA, considering these features specific for this particular polymer.

Turning to the energy details, since the relative MP2/6-31G(d) energies of those $C(sp^3)–C(sp^2)$ minima in PGA's model molecule (molecule II in Ref. [23]), which are included in the most populated regions Min1, Min2 and Min3 of the glycolide units, are rather similar, though somewhat larger for the (*trans*, *trans*) minimum (2.36, 0.0 and 0.48 kcal/mol, respectively [23]), and the barriers between these minima low, the population of the states is rather even. The relatively high population of the (t, t) region (Min1) is due to the packing effects, and related to the higher densities of PGA and PGA/PLLA in comparison with the PLAs (there are no (*trans*, *trans*) minima in the PLA's [23]). As regards the lactide units, the rotation about the $C(sp^3)–C(sp^2)$ bond in the model molecule of PLLA (molecule III in Ref. [23]) is energetically as feasible as that in PGA's model molecule, and therefore does not cause significant deviations to the distribution of the points along the C–C axis from that in the glycolide units. On the other hand, the *trans* region of the $C(sp^3)–O(sp^3)$ rotation is much less populated in PLLA (and in the PLLA/PDLAs) than in PGA (there are no *trans* minima for the $C(sp^3)–O(sp^3)$ rotation in PLLA [23]). The $C(sp^3)–O(sp^3)$ rotation in PLLA also is more restricted than the one in PGA. The g^+ minima are of larger relative energy than in PGA, and the barriers for transitions between the C–O g^- and g^+ states are high (in the order of 10 kcal/mol [23]). This makes the amorphous phase of PLLA somewhat more rigid than that of PGA, as can also be seen in Fig. 2. These energy features also explain the uneven population of the C–O g^+ and g^- states, the g^- regions being much more populated than the g^+ regions in the L-lactide units. The relative MP2/6-31G(d) energies, which for the (*, g^-) (* = any C–C conformation) minima in PLLA's model molecule are 0.0 and 0.30 kcal/mol, the energies of the (*, g^+) minima being 1.27 and 2.14 kcal/mol, also support the larger population of the (t, g^-) and (c, g^-) regions. This is expected to affect negatively, for example, diffusion of water molecules in PLLA, since the rigidity of the polymer matrix may hinder the opening of tunnels for diffusion.

The most significant differences in the populations between the copolymers and homo-polymers can be explained with the changes in intermolecular interactions. In order to consider intramolecular interactions, the potential energy surfaces were calculated in this work for the different combinations of three-monomer systems (LLL, LLD, etc.) using our modified PCFF. Those for the L-lactide units of the PLLA/PLLA/PLLA (LLL) and PGA/-PLLA/PGA (GLG) systems, and for the D-lactide units of the PLLA/PDLA/PLLA (LDL) and PLLA/PDLA/PDLA (LDD) systems are shown in Fig. 3. In the case of PGA/PLLA, the similarity of the LLL and GLG maps shows that the uneven population between the C–O g^+ states and the significant (10.4%) gain in the population of the (t, g^-) region cannot be explained on the basis of the intramolecular interactions alone. The 15.0% gain in the population of

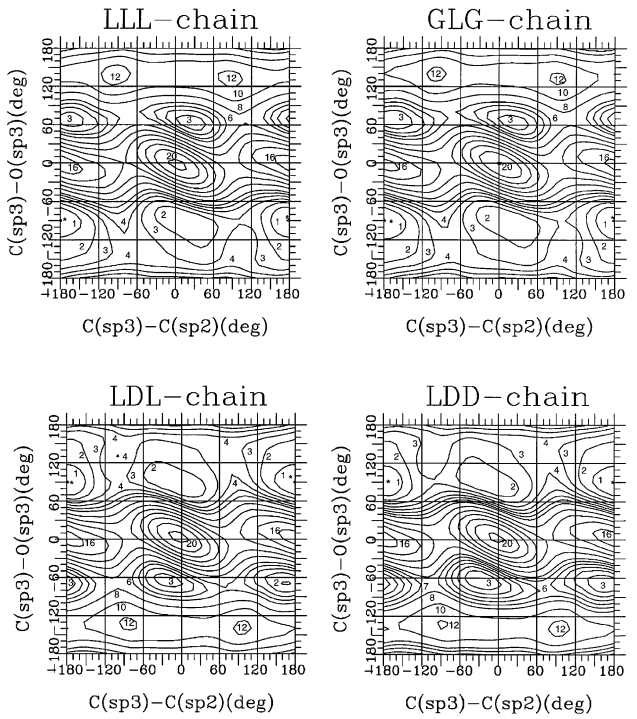

Fig. 3. Calculated potential energy surfaces of the LLL, GLG, LDL and LDD chains as a function of the $C(sp^3)–C(sp^2)$ and $C(sp^3)–O(sp^3)$ dihedral angles, as given by the modified PCFF [22,23]. Potential energy lines are shown at the 1 kcal/mol interval for energies ≤6 kcal/mol (in the LDD map for energies ≤8 kcal/mol), and at the 2 kcal/mol interval for energies >6 kcal/mol (in the LDD map for energies >8 kcal/mol), the potential energy of the global minimum being defined as zero (the global minima are marked with asterisks in the maps).

Table 4
Calculated solubility parameters (in $(J/cm^3)^{1/2}$) of PGA, PLLA, PLLA/PDLAs and PGA/PLLA

	Method	Solubility parameter
PGA	This study	34.0 ± 0.2
	QSPR[a,b]	23.82 (Fedors-like)
		19.28 (van Krevelen-like)
PLLA	This study	22.0 ± 0.2
Alternating PLLA/PDLA	This study	23.2 ± 0.2
Random PLLA/PDLA	This study	23.4 ± 0.1
	QSPR[a,b,c]	21.42 (Fedors-like)
		17.64 (van Krevelen-like)
Random PGA/PLLA	This study	26.6 ± 0.1
	QSPR[a,b]	22.43 (Fedors-like)
		18.32 (van Krevelen-like)

[a] MSI.
[b] QSPR does not take tacticity into account.
[c] The values are valid also for PLLA and alternating PLLA/PDLA.

the (t, g) regions in the L-lactide units of PGA/PLLA is thus a result from the influence of intermolecular interactions. The situation in alternating PLLA/PDLA is similar, and the LLL, LDL and LDD potential energy maps do not explain the differences seen in the populations of the D-lactide units of the random and alternating PLLA/PDLA copolymers. In alternating PLLA/PDLA, the C–O g^- states, and especially the (c, g^-) state, of the D-lactide units are much more populated than in the random polymer. These features also have to come from intermolecular interactions, which are significant enough to cause $C(sp^3)$–$C(sp^2)$ barrier crossings.

3.2. Probability of water uptake

3.2.1. Solubility parameters

The probability of water uptake in the studied polyesters was first considered by calculating the solubility parameters, given in Table 4. The respective values obtained by the QSPR method [33], which, however, only give a crude estimate of the solubility, are also given in Table 4. Since the QSPR method does not take tacticity into account the QSPR solubility parameters correspond to those of random copolymers. For the same reason, the values are the same for PLLA and the PLLA/PDLAs. There are two approaches in the QSPR method used [13]: Fedors-like [34] and van Krevelen-like [35], which mainly differ by parameterization of the correlation equations needed to predict the cohesive energies. The Fedors-like results are known to be somewhat larger for most polymers compared to the respective van Krevelen-like results [33]. This is also true for the polyesters studied here. The polyesters used in the parameterization of the QSPR method all have solubility parameters between 18 and 20 $(J/cm^3)^{1/2}$ [33], for which reason the QSPR method may fail in the case of PGA. It also has to be noted that solubility parameters for polyesters with non-isolated carboxyl groups, like the ones studied in this paper, have not been included in the parameterization of the QSPR method [33]. Thus, for a more reliable prediction of solubilities the parameters should be computed from the CEDs of the constructed amorphous models for those polymers, for which the QSPR method is not parameterized. Indeed, the solubility parameters calculated from the constructed amorphous models of the polyesters studied are larger than the values given by the QSPR method. For the PLAs all calculated solubility parameters are close to each other, whereas for PGA the values given by the QSPR method are only about two-third of the value calculated from the amorphous model.

The solubility parameter of PGA, as suggested also by the CEDs in Table 1, came out much larger but also closer to that of water (about 40 $(J/cm^3)^{1/2}$) than did those of the other polyesters. Water molecules could thus penetrate into PGA more easily than into the PLAs or PGA/PLLA. According to this, PGA would hydrolyze more easily than the other studied polyesters. The difference between the solubility parameters of PGA and the PLAs is clear (about 12 $(J/cm^3)^{1/2}$), indicating the strong effect of the PLAs hydrophobic methyl groups on the PLAs solubility. The difference is also large enough to be seen in water uptake by these polymers, and the result is in good agreement with the findings of Gilding and Reed [4], who noticed that the water uptake of GA/LA copolymers increase almost linearly in the amorphous range along with an increasing amount of the glycolic acid units in the copolymer. The solubility parameter of the (50%, 50%) PGA/PLLA, which was calculated close to the average values of PGA and PLLA, is in agreement with this finding, too. According to the QSPR results, instead, the water uptake would be very similar in the amorphous phase of all the studied polyesters.

3.2.2. Free volume

The packing of the generated amorphous structures, and how much room there is for water molecules in the amorphous phase, was investigated by first calculating free volumes. There are two methods that take the type of the penetrating small molecule into account in MSIs software for the analysis of free volume, i.e. the Gusev–Suter [36] and the Voorintholt [37] methods. In both methods, a uniform grid is introduced into the amorphous matrix. In the Gusev–Suter method, the Helmholtz free energy is computed at each grid point, which has a probe molecule. The interaction energy between the polymer matrix and the penetrant molecules is calculated using a Lennard-Jones 9-6 potential but neglecting the Coulomb interactions, which however may be very significant in materials with polar functional groups. The Voorintholt method, on the other hand, is based on a simple geometric algorithm where only the dimension of the penetrant molecule according to the van der Waals radius is taken into account (i.e. hard sphere-approximation). Both methods calculate the free volume based only on van der Waals interactions, though the Voorintholt method gives a more approximate estimate. However, the results of the Gusev–Suter method were found to be really sensitive to

the Lennard-Jones parameters used in the calculations. Since also the rigid matrix approximation in the Gusev–Suter method has been proved to be too crude in long-term dynamics simulations of small molecules in dense polymers [38], the Voorintholt method has to be used for these kinds of studies.

Thus, in the case of water molecules as penetrants, the maximum radius of the probe molecule in the Voorintholt calculations was set to 1.0 Å, and the distance between the grid points to 0.5 Å. The size of the water molecule is here taken to be smaller than the average dimension in different directions, based on the optimized geometry and van der Waals radii. In this way the flexibility of the polymer matrix can, to some extent, be taken into account. As in the Gusev–Suter method, the polymer matrix in the Voorintholt method is also constrained to be rigid, which may not be a valid approximation for flexible polymer chains. However, the flexibility of the polymer matrix in the Voorintholt method is further, at least partly, implicitly accounted for when assigning a gridpoint to the free volume region based on the probability (see equation (1) in Ref. [37]). On the other hand, the method does not make any distinction between polymer matrices with different flexibilities. Despite these approximations, the Voorintholt method is believed to give satisfactory results for comparison of free volumes in similar types of polyesters.

The distributions of the free volume in the studied polyesters using the Voorintholt method are given in Fig. 4. Only the volumes, which have a probability of 50% or higher to have room for the probe molecule of the given size, are shown in the picture. Examples of the free volume regions in the amorphous cells of PGA, PLLA and random PGA/PLLA are presented in Fig. 5. Since the free volume regions in PGA are very small, the cell is shown without the image chains. Based on Figs. 4 and 5, with the probe molecule mentioned earlier, amorphous PGA is most tightly packed, which is related to the unexpectedly high population of the (*trans*, *trans*) energy region (Table 3). Fig. 4 shows that there is somewhat more free space in the PLAs than in PGA, both small and large volume sites ((*trans*, *trans*) conformations are missing in the PLAs). Of the PLAs in alternating PLLA/PDLA, there are more small volume sites but less large ones than in the other PLAs, which may be negative regarding the water uptake by this particular polymer. The results for PGA/PLLA again are closer to those of PLLA and of its other studied copolymers than of PGA. A common feature of the studied polyesters is that the free volume regions are more or less separate small volume pockets, which may prevent the water molecules to move freely in the polymer matrix. In this kind of systems, the possibility to account for the flexibility of the polymer matrix in the simulations becomes even more important when studying diffusion of small molecules. Adding less rigid glycolide units into PGA/PLLA would probably positively affect the diffusion, though the free volume results show PGA having less space for water molecules than what the PLAs do. The Voorintholt method may thus underestimate the actual free volume in PGA as compared to PLA due to the rigid matrix approximation and the less rigid $C(sp^3)–O(sp^3)$ rotation of the PGA chains versus the PLA chains. In any case, these results only show that the packing in the amorphous phase of the studied polyesters does not vary much in the different systems, thereby also yielding similar probabilities for water uptake. The Voorintholt method does neither give any information about the environment of the free space, such as the free

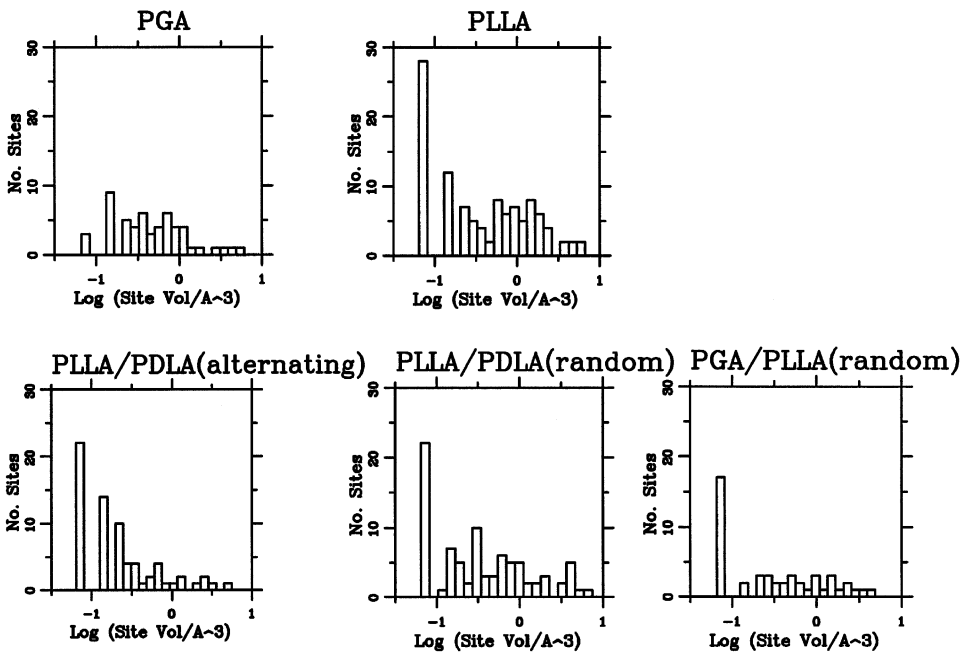

Fig. 4. Calculated Voorintholt free volumes in PGA, PLLA, PLLA/PDLAs and PGA/PLLA.

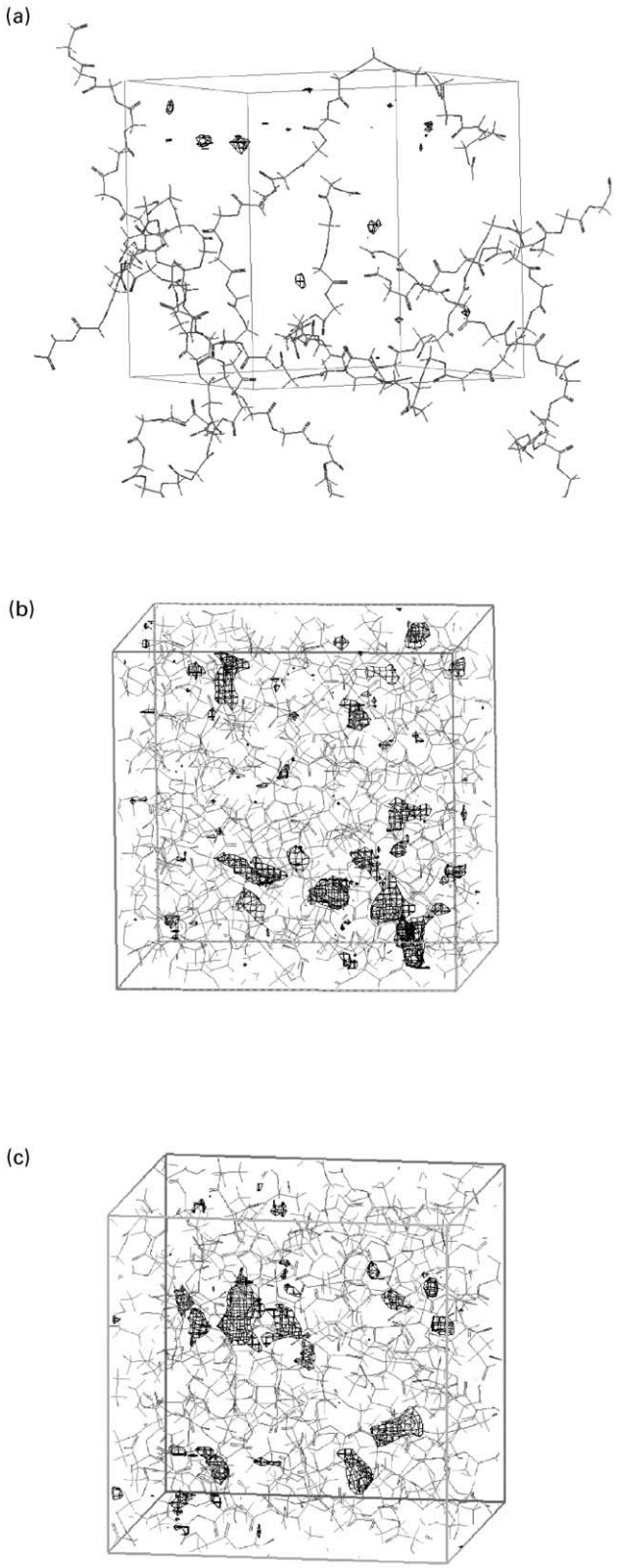

Fig. 5. Distribution of the free volume regions in a central cell of (a) PGA, (b) PLLA, and (c) random PGA/PLLA as calculated with the Voorintholt method. For PGA the cell is shown without image molecules due to the small size of the free volume regions.

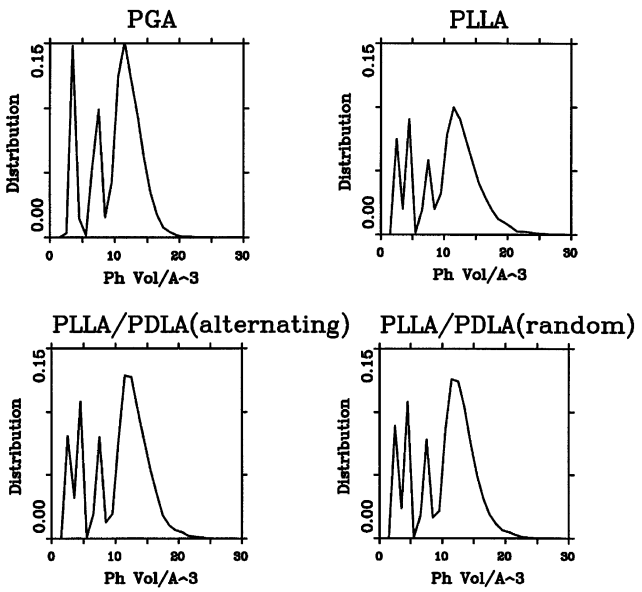

Fig. 6. Calculated distributions of the Voronoi polyhedra in PGA, PLLA and PLLA/PDLAs.

space in the hydrophilic or hydrophobic regions of a polymer.

The relative free volume distribution can also be estimated by constructing Voronoi tessellations [13,39] and by examining their statistics. In the Voronoi method, a Voronoi polyhedron, related to the available free space, is constructed around a center atom, and the distribution of polyhedra with various shapes and sizes is generated to give information about the free space regions. These distributions are shown in Fig. 6 for PGA and the PLAs. The largest fraction of polyhedra has the size of 8.5–25.0 $Å^3$, which corresponds to the space in which the water molecules fit well. Of the available free space 68% belongs to this particular region in all polyesters studied in this paper. As regards the absolute amounts of the free volume sites of the size 8.5–25.0 $Å^3$, it is slightly smaller for PGA (4.45 $Å^3$) than for PLLA (5.65 $Å^3$) or the PLLA/PDLAs (5.23–5.34 $Å^3$). The Voronoi method, too, shows that the packing of the studied polyesters is similar, though PGA seems to have slightly less free volume as compared to the PLAs. Here, too, the flexibility of the polymer matrix may change the situation by the opening of tunnels for water molecules. This, however, cannot be studied with the methods used.

3.2.3. Pair correlation functions

PCFs, which also give information about packing of the atoms in a cell, were computed for PGA and the PLAs. Both inter- and intramolecular PCFs were calculated for the carbonyl oxygen atom with respect to all other atoms of the system, since the hydrolysis in polyesters starts with proton transfer to the carbonyl oxygen atom of the ester group. The intra- and intermolecular PCFs for PGA, PLLA and the PLLA/PDLAs are given in Fig. 7, and the most distinct

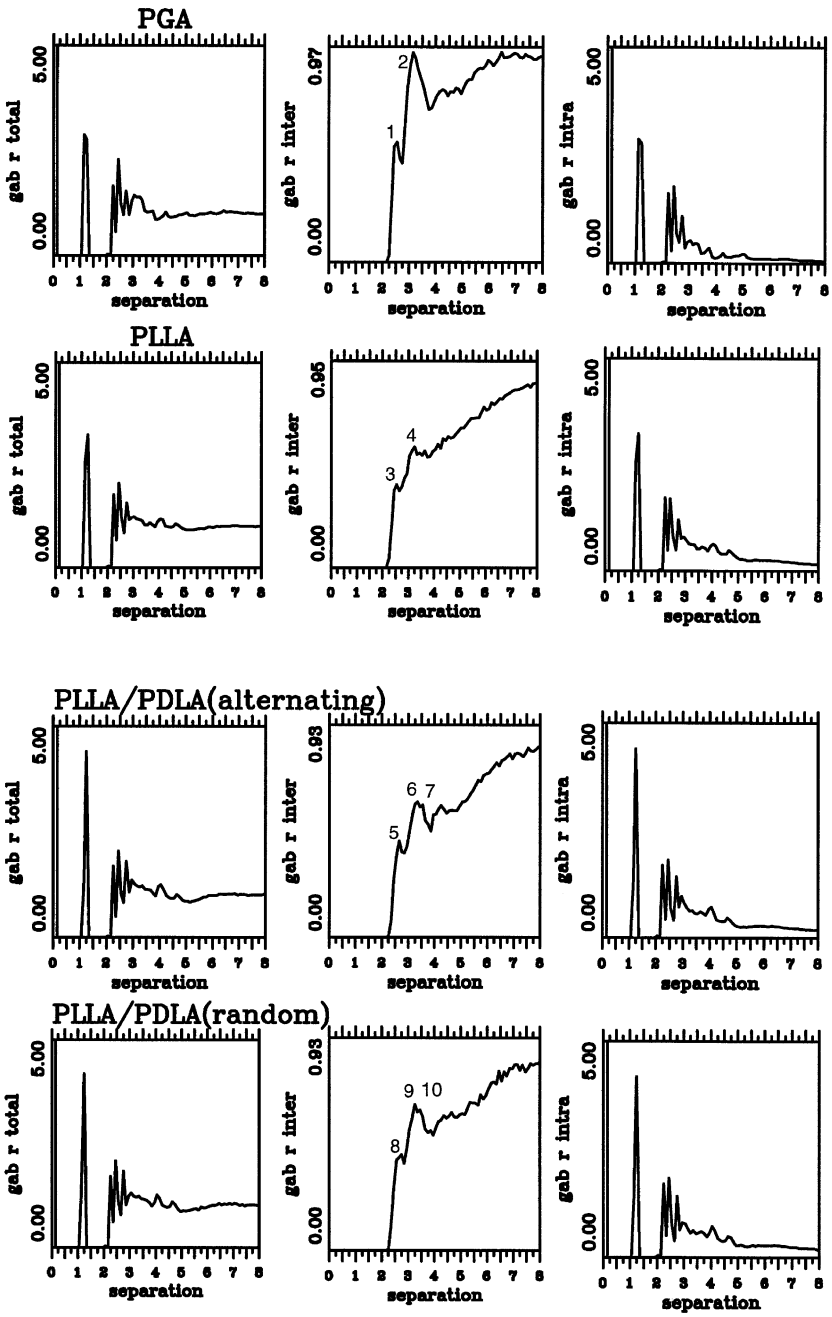

Fig. 7. Calculated intra- and intermolecular PCFs for C=O···X (X = any atom) contacts in PGA, PLLA and PLLA/PDLAs.

peaks are listed in Table 5. In all intermolecular PCFs, there are peaks at ~2.55–2.65 Å corresponding to C=O···H distances, and at ~3.15–3.25 Å corresponding to C=O···O=C distances. In the PLLA/PDLAs the latter peak is split, with the second component at 3.55 Å. In PGA there is a shoulder at about 3.5 Å. These can be compared to the sums of the van der Waals radii, which for O···H is 2.6 Å and for O···O 2.8 Å [40]. The results are very similar in all studied polyesters, which show that there are no significant differences in the packing of pure amorphous structures, which could lead to different water uptake of the particular polyesters. As regards the intramolecular PCFs, the most prominent peaks correspond to typical bond lengths and 1,3-distances (valence angles) [22,23] as well as to non-bonded atom–atom distances in local minimum energy conformations of the studied polymer chains. The peaks for bonded 1,4-distances (torsions) are broad due to the shallowness of the energy minima [22,23] (Fig. 2).

The effect of water on the packing of the cells in the amorphous phase of all studied polyesters was considered by calculating the intermolecular PCFs with 10 H_2O molecules included in the refined amorphous cells. Two additional cycles with 1000 MM and 15 000 MD steps, and

Table 5
Calculated C=O···X (X = any atom) distances (in Å) and intensities *I* (in arbitrary units) of PGA, PLLA and PLLA/PDLAs

	Peak[a]	Separation	*I*
PGA	1	2.55	0.54
	2	3.15	0.95
PLLA	3	2.55	0.38
	4	3.25	0.55
Alternating PLLA/PDLA	5	2.65	0.42
	6	3.25	0.58
	7	3.55	0.58
Random PLLA/PDLA	8	2.65	0.40
	9	3.25	0.64
	10	3.55	0.61

[a] Numbering of peaks in Fig. 7.

Table 6
Calculated intermolecular C=O···H–OH distances (in Å) and intensities *I* (in arbitrary units) of PGA, PLLA, PLLA/PDLAs and PGA/PLLA

	Peak[a]	Separation	*I*
PGA	1	1.85	3.95
	2	3.25	1.51
PLLA	3	1.95	5.76
	4	2.95	1.86
Alternating PLLA/PDLA	5	1.85	7.79
	6	3.25	1.80
Random PLLA/PDLA	7	1.85	7.79
	8	3.15	1.92
Random PGA/PLLA	9	1.85	5.47
	10	3.05	2.01

[a] Numbering of peaks in Fig. 8.

a final energy minimization, were carried out to optimize the cells with the water molecules. (As a test six such cycles were performed on one cell of PLLA, but the results for the cell were practically unchanged after the second cycle.) The PCFs, calculated for the distances between the hydrogen atoms of the water molecules and the carbonyl oxygen atoms of the polyester chains, are presented in Fig. 8 and the peaks in Table 6. The general shape of the PCFs is similar for all polyester/water combinations. The corresponding peaks are located at about the same distances, but the intensities of the peaks that give the number of H···O contacts differ somewhat. The sharp peak at about 2.0 Å indicates the shortest length of the hydrogen bond formed between one of the hydrogen atoms of the water molecule and the carbonyl oxygen atom of the polyester chain. A peak at about 3.0 Å is related to the longer distance between the other hydrogen atom of the H_2O molecule and the carbonyl oxygen atom. The peak at about 2.0 Å is lowest for PGA and highest for the PLLA/PDLAs, the intensities of the peaks for PLLA and PGA/PLLA being about the same and between the two extremes. This indicates that there are more water molecules at the hydrogen bond distance from the carbonyl oxygen atoms in PLLA and its copolymers than in PGA. A possible explanation for this is the presence of hydrophobic methyl groups in the PLAs, which force the water molecules closer to the carbonyl oxygen atoms than in PGA, which has no methyl side groups.

In all polymers studied in this paper, the $C(sp^3)$–$C(sp^2)$ rotation takes place easily in both the lactide and glycolide units (Figs. 2 and 3). Therefore, the possible protective steric effect of the methyl groups in the lactide units against hydrolysis is insignificant. This is in agreement with the observation by Fredericks et al. [10] that in the actual degradation of GA/LA copolymers, the

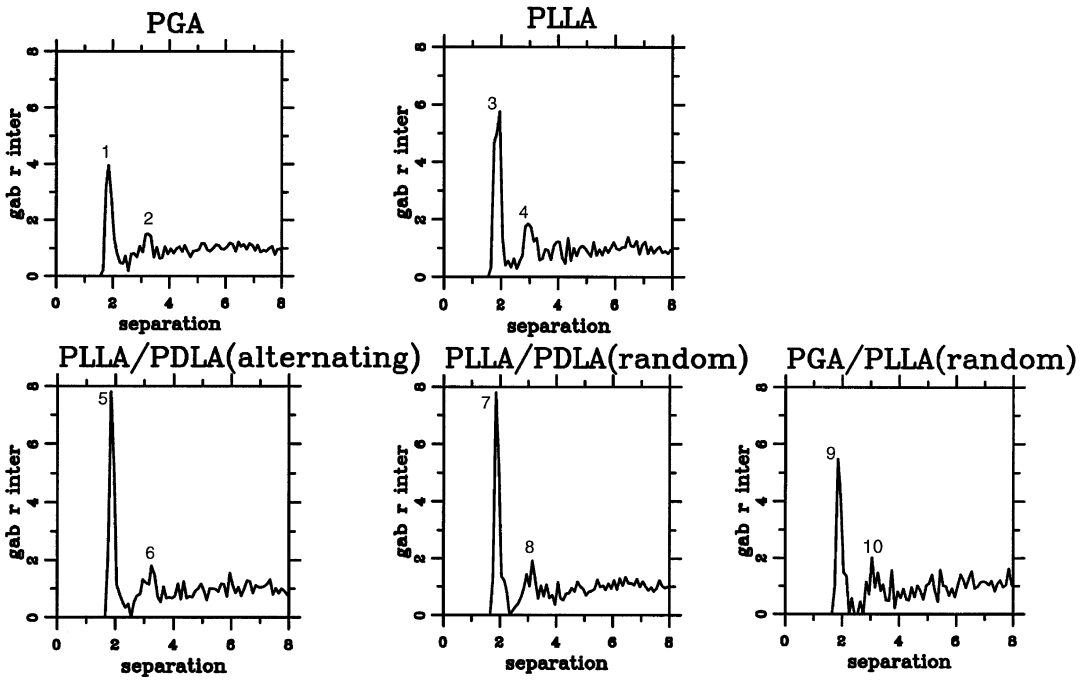

Fig. 8. Calculated intermolecular PCFs for C=O···H–OH contacts in the studied polyesters.

lactide/glycolide ratio remained constant during the hydrolysis.

4. Conclusions

According to this study, the main factor controlling the probability for water uptake in the amorphous phase of the studied polyesters is the number of hydrophobic groups, which affects both the solubility parameter and the PCFs when water molecules are present in the cells. In PGA, there are fewer hydrophobic groups than in PLA or its copolymers. All other calculated properties, which could affect water uptake, came out rather close to each other.

The solubility parameter, as calculated from the CEDs of the generated amorphous structures, suggested that, in agreement with experiments, of the studied polyesters PGA is most compatible with water, whereas PLLA is least compatible. The difference (about 12 $(J/cm^3)^{1/2}$) between the solubility parameters of PGA and PLLA is large enough to explain the experimentally observed increase in water uptake of amorphous PGA/PLA as a function of increasing amounts of glycolic acid [4]. On the other hand, when using the QSPR method with the present parameterization [33], care should be taken when predicting solubility for the kinds of polyesters studied in this paper. The QSPR values, as compared with those obtained from the constructed amorphous models, are systematically smaller, especially for PGA, and the slight differences between them, about 1–2 $(J/cm^3)^{1/2}$, would suggest a very similar ability of all the studied polyesters to absorb water.

The distributions of the free volume calculated by the Voorintholt method suggested that PGA is more tightly packed than the other studied polyesters, PLLA and its copolymers having a larger number of separate small volume sites, which partly also are larger in size than those in PGA. Due to the rigid matrix approximation in the method, the free space in PGA may, however, be underestimated. The distributions of the Voronoi tessellations revealed that the amount of free volume in the region, in which the water molecules fit well, is only slightly smaller for PGA than for PLLA or the PLLA/PDLAs. Simulations with water molecules in the cells predicted that the number of hydrogen bonds formed between the water molecules and the carbonyl groups of the chains was largest for the PLLA/PDLAs, the numbers for PLLA and PGA/PLLA being somewhat smaller, and smallest for PGA. The main reason for this is most probably the effect of hydrophobic methyl groups in the PLAs and PGA/PLLA, which force more water molecules closer to the ester groups in PLA than in PGA.

In addition to the hydrophilic/hydrophobic balance, the local flexibility of the chains affects the water uptake of a polymer. The distributions of the adjacent chain ($C(sp^3)$–$C(sp^2)$, $C(sp^3)$–$O(sp^3)$) dihedral angle pairs, together with the potential energy surfaces, given in Figs. 2 and 3, show that the PGA chain is locally most flexible. The PGA/PLLA chains show somewhat smaller flexibility, the PLLA and the PLLA/PDLAs having the least chain flexibility, though still in a significant amount. The rotation about the $C(sp^3)$–$C(sp^2)$ bonds, however, takes place easily in both the lactide and glycolide units, reducing the protective steric effect of the methyl groups of the lactide units against hydrolysis. This explains the observation of Fredericks et al. [10] that in the actual degradation of copolymers, the lactide/glycolide ratio remained constant during hydrolysis.

An interesting feature in the studied copolymers is that in random PGA/PLLA, the glycolide units affect significantly the population of the L-lactide units but not vice versa. Also in alternating PLLA/PDLA, the presence of L-lactide units change the population of the D-lactide units but not vice versa, whereas no such large differences between the L and D populations are seen in random PLLA/PDLA. These facts cannot be explained by intramolecular interactions alone due to the similarities in the potential energy surfaces of the different three-monomer systems, calculated to give information about the energy behavior of the chains in the studied polymers. The intermolecular interactions thus have to be significant enough to cause the particular variations in populations.

Acknowledgments

The Neste Foundation (J.B.) is gratefully acknowledged for financial support. Thanks are also due to Dr Kim Palmo and MSc Virpi Korpelainen for comments on this paper. We thank the Center for Scientific Computing (Espoo, Finland) for computational resources.

References

[1] Kister G, Cassanas G, Vert M. Polymer 1998;39:267–73.
[2] Chiellini E, Solaro R. Adv Mater 1996;8(4):305–13.
[3] King E, Cameron RE. J Appl Polym Sci 1997;66:1681–90.
[4] Gilding DK, Reed AM. Polymer 1979;20:1459–64.
[5] Chu CC. J Appl Polym Sci 1981;26:1727–34.
[6] Reed AM, Gilding DK. Polymer 1981;22:494–8.
[7] Mark HF, Bikales NM, Overberger CG, Menges G, Kroschwitz JI, Encyclopedia of polymer science and engineering, vol. 2. Canada: Wiley; 1985.
[8] Li S, Vert M. Polym Int 1994;33:37–41.
[9] Li S, Vert M. Macromolecules 1994;27:3107–10.
[10] Fredericks RJ, Melveger AJ, Dolegiewitz LJ. J Polym Sci, Polym Phys Ed 1984;22:57–66.
[11] Schindler A, Harper D. J Polym Sci, Polym Chem Ed 1979;17:2593–9.
[12] Hiljanen-Vainio M, Varpomaa P, Seppälä J, Törmälä P. Macromol Chem Phys 1996;197(4):1503–23.
[13] InsightII, 4.0.0.P and Polymer 10.0; April 1998. San Diego: MSI 1998 (now Accelrys, Inc.).
[14] Hwang MJ, Stockfisch TP, Hagler AT. J Am Chem Soc 1994;116:2515–25.
[15] Peng ZW, Ewig CS, Hwang MJ, Waldman M, Hagler AT. J Phys Chem A 1997;10:7243–52.
[16] Sun HJ. J Comput Chem 1994;15:752–68.

[17] Sun H. Macromolecules 1994;26:5924–36.
[18] Sun H, Mumby SJ, Maple JR, Hagler AT. J Am Chem Soc 1994;116:2978–87.
[19] Sun H. Macromolecules 1995;28:701–12.
[20] Sun H, Mumby SJ, Maple JR, Hagler AT. J Phys Chem 1995;99:5873–82.
[21] Sun H, Rigby D. Spectrochim Acta A 1997;53:1301–23.
[22] Blomqvist J, Ahjopalo L, Mannfors B, Pietilä L-O. J Mol Struct (Theochem) 1999;488:247–62.
[23] Blomqvist J, Mannfors B, Pietilä L-O. J Mol Struct (Theochem) 2001;531:359–74.
[24] Fletcher DA, McMeeking RF, Parkin D. The United Kingdom chemical database service. J Chem Inf Comput Sci 1996;36:746–9.
[25] Blomqvist J, Pietilä L-O, Mannfors B. Polymer 2001;42:109–16.
[26] Blomqvist J. Polymer 2001;42:3515–21.
[27] Honeycutt JD. Comput Theor Polym Sci 1998;8:1–8.
[28] Theodorou DN, Suter UW. Detailed molecular structure of a vinyl polymer glass. Macromolecules 1985;18:1467–78.
[29] Theodorou DN, Suter UW. Atomistic modeling of mechanical properties of polymeric glasses. Macromolecules 1986;19:139–54.
[30] Allen MP, Tildesley DJ. Computer simulation of liquids. Oxford: Oxford University Press; 1987.
[31] Epple M, Hergberg O. J Mater Chem 1997;7(6):1037–42.
[32] Grijpma DW, Pennings JP, Pennings AJ. Coll Polym Sci 1994;9:1068–81.
[33] Bicerano J. Prediction of polymer properties. New York: Marcel Dekker; 1993.
[34] Fedors RF. Polym Engng Sci 1974;14:147–54, see also page 472.
[35] van Krevelen DW. Properties of polymers, their estimation and correlation with chemical structure. Amsterdam: Elsevier; 1976.
[36] Gusev AA, Suter UW. Dynamics of small molecules in dense polymers subject to thermal motion. J Chem Phys 1993;99:2228–34.
[37] Voorintholt R, Kosters MT, Vegter G, Vriend G, Hol WGJ. J Mol Graphics 1989;7:243–5.
[38] Gusev AA, Arizzi S, Suter UW, Moll DJ. J Chem Phys 1993;99:2221–7.
[39] Voronoi MG. J Reine u Angew Math 1908;134:198–287.
[40] Vilkov LV, Mastryukov VS, Sadova NI. Determination of the geometrical structure of free molecules. Moscow: Mir; 1983.